HSPI The Open Access Publisher

ANNALS OF CIVIL AND ENVIRONMENTAL ENGINEERING
ISSN 2574-0350

Research Article

Improving the Concrete Compressive and Flexural Strength with a Low Fraction Addition of Carboxylated Nitro-oxidized Cellulose Nanofibrils from Banana Rachis

Ngesa Ezekiel Mushi* and Emmanuel Kagya

Department of Mechanical and Industrial Engineering, College of Engineering and Technology, University of Dar es Salaam, P.O.BOX 35131, Dar es Salaam, Tanzania

Abstract

Conventionally, concrete strength depends on the bonding interface, especially in hydrated products such as calcium silicate hydrate (CSH). As a result, concrete is sensitive under tensile load. With its unique properties, a low fraction of carboxylated nitro-oxidized cellulose nanofibrils (NOCNF) from the banana rachis is employed to improve the mechanical performance of the concrete nano structurally. Compressive and flexural strength using the NOCNF content at 0, 0.05, and 0.1 wt. % cured in 7 and 28 days were evaluated. Notably, the compressive strength increased by 16% and flexural strength by 13% at 0.1% NOCNF compared to plain concrete after the 28 curing days. A low NOCNF fraction achieved a good, albeit impossible, performance with the microscale fibers. The nanostructured effect was discussed twofold: an excellent interaction between the NOCNF and the hydrated products and the carboxylic groups on the NOCNF surface enhanced the cement hydration. These data are better than the literature based on the small-diameter cellulose nanofibrils without the carboxyl groups. As a sustainable nanocomponent, NOCNF could be a perfect candidate to improve concrete performance under mechanical load.

More Information

***Address for correspondence:** Ngesa Ezekiel Mushi, Department of Mechanical and Industrial Engineering, College of Engineering and Technology, University of Dar es Salaam, P.O.BOX 35131, Dar es Salaam, Tanzania, Email: mushi.ngesa@udsm.ac.tz

https://orcid.org/0000-0002-1848-6120

Submitted: September 05, 2024
Approved: September 16, 2024
Published: September 17, 2024

How to cite this article: Mushi NE, Kagya E. Improving the Concrete Compressive and Flexural Strength with a Low Fraction Addition of Carboxylated Nitro-oxidized Cellulose Nanofibrils from Banana Rachis. Ann Civil Environ Eng. 2024; 8(1): 087-095. Available from: https://dx.doi.org/10.29328/journal.acee.1001072

Keywords: Banana rachis; Concrete; Carboxylated nitro-oxidized cellulose nanofibrils; Compressive strength; Flexural strength

Check for updates

OPEN ACCESS

Introduction

The mud, grasses, stones, animal hides, or timber structures were once a luxury. Recently, concrete has dominated the building industry. Concrete is a multiphase ceramic composite of aggregates dispersed in a cementitious matrix. Predominantly, the Calcium–Silicate–Hydrate (CSH) nanoparticles constitute a primary hydration product of the cement. The CSH accounts for more than 60% of the cement hydration products and provides the bonding interface essential for strength [1]. Concrete is especially strong under compression load. The concrete is heavy and very brittle, which is somewhat of a disadvantage. Porosity may be problematic [2]. Brittleness is mainly expressed in the load structures under fatigue, impact, uniaxial tension, or flexural deformation [3]. Traditionally, concrete is reinforced with steel ribbed bars to supplement load under tension, flexural, or shear. The natural fibers from non-woody plants such as banana, sisal, coconut fibers, straws, bamboo, or pine leaves could mixed with the concrete to impact some ductility. These plant fibers are strong and flexible, biodegradable, renewable, and environmentally friendly, aligning with the global initiative on sustainability. They come in microscale sizes. For example, it was reported that a 5 wt.% banana fibers improved concrete mechanical properties - up to 80% increase in flexural and compressive strength [4].

Recently, Cellulose Nanofibrils (CNF) have gained attention as a reinforcement nanocomponent in cementitious matrices. A 26% enhancement in compressive strength from about 74 MPa to 93 MPa at 0.05 wt.% cellulose filaments (CF) was observed by incorporating mechanically treated CF of diameter 30 – 400 nm from wood [5]. Moreover, a 20.6% increase in flexural strength from 4.84 MPa to 5.84 MPa at 0.2% CF nanofibril fraction was reported [5]. In addition, a 0.04 wt.% of commercial Microcrystalline Cellulose (MCC) from cotton resulted in a 10.68% increase in compressive strength, from about 46 MPa to 51 MPa, and a 25% increase in flexural strength from about 122 MPa to 152 MPa [6]. Higher content co. 5 wt.% of CNF from Cladophora algae with a diameter of 37

nm - 55 nm resulted in a 170% increase in flexural strength, from 2.21 MPa to 5.96 MPa [7]. The nanofibril reinforcement is remarkable compared to the 5 wt.% microscale fibers from bananas. Essentially, the reinforcing mechanism is complex. A hydration mechanism was suggested, correlating concrete strength to the presence of CSH nanoparticles. A cementitious matrix observes a similar phenomenon [1]. The CNFs primarily act as a water duct, promoting hydration in capillaries or regions previously occupied by anhydrous cement particles, such as calcium oxide-silicon oxide [8]. The CSH nanoparticles are also uniformly distributed in the cement matrix, reducing the porosity. There are still limited studies on the mechanical performance of concrete structures reinforced with CNFs. The previous works mainly reported on concrete composites containing sand and cement. In this study, concrete constitutes cement, fine aggregates or sand, and coarse aggregates or gravel. The aggregate's chemical composition is limestone and silicate. Only Barnat-Hunek, et al. [9] probably worked on such concretes. Concurrently, a significant improvement in concrete mechanical properties was observed using CNFs from apple wastes-a 1 wt.% of CNFs with an average diameter of 2.68 nm resulted in a 23.3% increase in compressive strength from 38.8 MPa to 43.7 MPa and a 34.5% increase in flexural strength from 4.23 MPa to 5.69 MPa [9]. These data are impressive compared to those from microscale fibers or the microscale filaments with a higher fiber fraction.

Notably, the primary role of cellulose nanocrystals in the plant cell wall also inspired this study – though biological structures achieve these robust mechanical properties through a hierarchical organization. Cellulose is a β - 1, 4 - glucan in an extended polymer chain conformation. The properties of CNFs are superior to those of microscale fibers, for example, banana fibers (tensile strength = 550 MPa, stiffness = 3.5 GPa) [10]. The stiffness of cellulose crystal (110 - 220 GPa) competes with those of the stiffest synthetic fibrils, such as carbon (150 - 500 GPa) and Kevlar (124 - 134 GPa) [11]. Nanostructurally, the high stiffness may be correlated to the excellent toughness of biological structures [12].

Banana rachis fiber predominantly comprises 31 – 49 wt.% cellulose, 16 – 38 wt.% hemicellulose, and 6 – 12 wt.% lignin [13,14]. Nitro-oxidation facilitates CNF isolation mechanochemically [15]. Nitroxonium ions attack the hydroxyl group at the C6 position, the hydroxonium ion introduces the carboxyl groups, and lignin and hemicelluloses are removed from the cell wall [16]. The process is cheap and environmentally friendly. The carboxyl and hydroxyl groups presumably initiate the CSH growth nano structurally [17]. Hydroxyl radicals are powerful oxidizing agents everywhere, and their presence in the surroundings is undesirable [18]. Incorporating the CNF into the concrete may be essential for scavenging the hydroxyl radicals.

As stated, nanofibrils impact concrete's mechanical properties differently than plant fibers—a higher CNF fraction, such as 5 wt.% from Cladophora or the 1 wt.% from Apple has already shown remarkable results [7]. The nanofibrils were not oxidized, albeit had no carboxylic groups. This study investigates a lower fraction (0.05 and 0.1 wt.%) of carboxylated Nitro-Oxidized Cellulose Nanofibrils (NOCNF) in addition to the mechanical properties of concrete. The main objective is to understand the effect of the carboxylated nanofibrils, the oxidized cellulose nanofibrils, from biomass waste on the compressive and flexural strength of the concrete. The previous study reported on the wettability and adhesive properties of the CNF on the concrete properties [9]. Concrete mechanical properties strongly correlate to the hydration process is crucial, and the hydrophilic characteristics of the nanofibrils are expected to be favorable for the formation of CSH nanoparticles. Additionally, concrete is very porous, and the nanoscale size of the nanofibrils is good for filling the micro and nano-voids, creating a better cementitious interface. The future of eco-friendly building structures has potential, and employing CNF has an impact because of its low carbon footprint.

Materials and methods

Materials

Fine (sand) and coarse aggregates (gravel from rocks) were obtained from local suppliers in Tanzania along the coast of East Africa. White natural sand of particle size below 5 mm, moisture content of 0.01%, a specific gravity of 2.6 g/cc, and fineness modulus of 2.53 was used as a fine aggregate. The black coarse aggregates particle ranged from 5 to 20 mm, with a moisture content of 0.05%, specific gravity of 2.6 g/cc, and fineness modulus of 5.9. In addition, an ordinary Type II Portland cement (CEM II/ A-L 42.5N, Twiga Cement) was used. The NOCNF was extracted from Banana rachis through nitro–oxidation [15].

Physical properties of the NOCNFs

The degree of oxidation was 0.455 mmol/g by conductometric titration, and the nanofibril diameter of 5.2 nm and length of 1.23 μm were reported using a Transmission Electron Microscope (TEM) (Hitachi, Japan). The TEM imaging procedure was reported previously [19]. A 5 gm of cement was dissolved in 20 ml of deionized water to examine cement dissolution and monitor interaction with the NOCNFs of a 1 wt.% was then added to the solution in volume fractions of 5, 10, and 30%, vigorously shaken for a minute, and left overnight.

Preparation of the NOCNF concrete mixture

The mixed proportions of sand, coarse aggregates, water, and cement by weight were prepared as summarized in Table 1. The mix proportions by weight, such as cement, water, sand, aggregate, or gravel, was 100:48:200:300 for plain concrete's assumed target strength of 32 N/mm2 (N32

Table 1: A proportional mix composition of sand, coarse aggregates, cement, water, and NOCNF in the concrete mixture.

Concrete sample	Cement (kg/m^3)	Sand (kg/m^3)	Aggregate (kg/m^3)	Water (kg/m^3)	NOCNF (kg/m^3)
0 % NOCNF	375	637.3	1133.1	180	0
0.05 % NOCNF	375	637.3	1133.1	180	1.875
0.1 % NOCNF	375	637.3	1133.1	180	3.750

concrete grade). Three concrete mixtures were prepared - two samples of 0.05% and 0.1% (wt.% of cement) NOCNF and a reference sample with 0% NOCNF as a control. Energy-dispersive X-ray (EDX) determined the chemical composition of the plain concrete. The main elements reported included silicon, calcium, aluminum, iron, and potassium; see results in Table 2. An electron beam with an energy of 15 keV struck the sample's surface to emit X-rays.

Workability of the concrete mixture by slump test

A slump test measured the consistency of fresh concrete. The slump test was done using a frustum of a slump cone mold with a 30 cm height, top diameter of 10 cm, and bottom diameter of 20 cm, with a tamping rod of 16 mm diameter and 600 mm long. The concrete samples were mixed for 5 min. The slump flow was recorded manually for 0%, 0.05%, and 0.1% NOCNF content.

Mechanical characterization of the NOCNF concrete mixture

The concrete samples were prepared according to the standard method of making and curing test specimens [20]. The concrete cubes of 150 x 150 x 150 mm^3 (Figure 1A,B) were prepared for the compressive strength test. The compression test was performed using the Universal Tensile model UTM 200T (Daewoo Engineering, Korea). The compressive strength was recorded from the load overextension. Concrete prisms of dimensions shown in Figure 1C,D were prepared for the flexural test. The flexural strength was determined using a four-point bend test where the loading span is 1/3 of the support span using the Universal tensile machine model UTM 200T (Daewoo Engineering, Korea). The flexural strength was recorded at fracture. The samples for compression and flexural tests were cured under water for 7 and 28 days. The porosity of the concrete samples was measured based on the density method using Eq. (1). The concrete shrinkage was determined from the change in length of a concrete sample when dried from about its liquid limit, expressed as a ratio of the initial length shrinkage of 0.1 wt.% NOCNF and the plain concrete samples were monitored over 21 curing days.

$$Porosity = \left[1 - \frac{Density\ of\ concrete\,(with\ pores)}{Density\ of\ samples(without\ pores)}\right] \times 100\% \quad (1)$$

X-ray powder diffraction analysis

The crystal structures of the NOCNF, plain concrete, and 0.1% NOCNF concrete mixtures cured after 28 days were examined. The NOCNF film was prepared and then attached

Table 2: Elemental composition of the plain concrete mixture.

Element	Composition (%)
Silicon, Si	48.040
Calcium, Ca	28.538
Aluminum, Al	15.196
Iron, Fe	5.256
Potassium, K	0.502

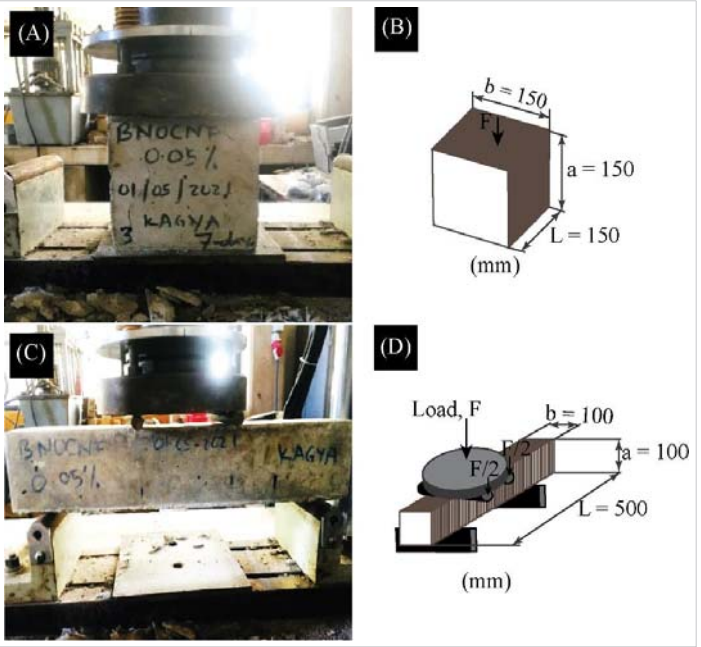

Figure 1: A compression and flexural strength test setup (A) Image of a compression cube loaded under compression test (B) A compression cube dimensions (C) Image of a rectangular prism under the flexural test setup (D) A schematic diagram of four-point bend test and dimensions of a flexural rectangular prism.

to the sample holder with masking tape. The concrete samples, including sand and gravel, were crushed to powder for analysis. The X-ray Powder Diffraction (XRD) patterns were collected in the 2θ range of 5^o – 45^o using an X-ray diffractometer (Rigaku Co., Ltd., South Africa) with Cu Kα radiation (λ = 1.5418 Å) at 40 kV and 40 mA.

Results and discussions

Hydrocolloid suspension of cement particles and NOCNF

Figure 2A shows the TEM image characterizing the nanofibrils. The structural information is published elsewhere [19]. Notably, the nanofibrils are thin and micrometers long- a 1 wt.% of the NOCNF hydrogel is presented in the extract image; see Figures 2A,2B is the visual inspection of a hydrocolloid suspension of NOCNF-cement mixture in glass vials. The cement particles and NOCNF were shaken to monitor the hydrocolloid stability of the cement particles. Initially, the cement particles partially dissolved in the absence of NOCNF. The dissolved particles (mainly CaO) appear brownish in the supernatant. Then, the cement particles gradually stabilized with the addition of the NOCNF content. The nanoscale properties, including the presence of the carboxylic groups, of the NOCNF are responsible for

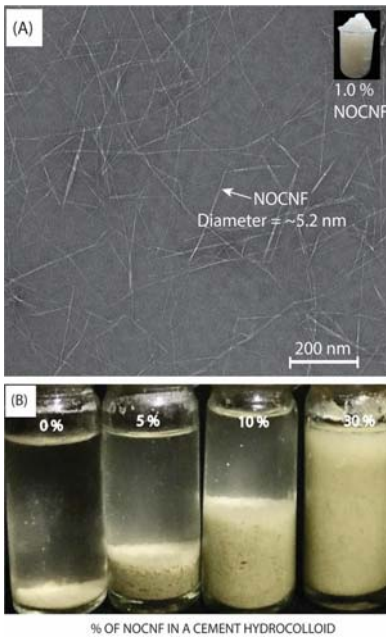

Figure 2: NOCNF-Cement particle hydrocolloid mixture (A) A TEM image of the NOCNF at high resolution. An insert is a photographic image of 1.0 wt. % NOCNF suspension in a test tube (B) A hydrocolloid suspension of 0%, 5%, 10%, and 30 wt. % NOCNF content dispersed in a cement particles (5 µm) hydrocolloid.

the cement particle stabilization observed in Figure 2B. The nanofibrils are long and slender, essential for entanglements in the suspension. The carboxylic groups may be stable even over a wide pH range. Predominantly, the cement particles contain calcium oxide and silicon oxide [1,17]. In principle, hydrated products such as CSH or CH precipitation begins once the cement particles dissolve in water. A supersaturation initiates nucleation and growth [17]. The observed particles at 0% NOCNF are from the undissolved cement particles, probably the SiO.

Workability of the NOCNF concrete paste

The bar chart in Figure 3A presents the slump flow of the NOCNF concrete and the reference material. The slump cone filled with the concrete mixture was slowly lifted, eventually recording the slump flow; see the cone and the concrete in Figure 3B. From the image, the slump flow corresponds to the height reduced, as observed from the arrow. The decrease is remarkable at a low fraction addition of NOCNF. For example, the slump height decreased by 40.8% at 0.05 wt.% fraction (slump flow = 80 mm) compared to the reference sample at 0% (slump flow = 130 mm). The insignificant slump change for 0.05% and 0.1% samples in Figure 3A is difficult to understand. Concrete workability depends on water-to-cement ratio, mixing design ratios, size and grading of aggregates, and use of admixtures or supplementary cementitious materials. The slump results are consistent with previous findings by Hisseine, et al. [5]. Up to 300% slump flow was reduced using 0.3 wt.% wood cellulose filaments, a somewhat higher addition of larger nanofibrils (diameter ≈ 400 nm). Moreover, the data support observing those from the hydrocolloid presented in Figure 2B. One possibility is that the rich content of surface hydroxyl and carboxylic groups allows for a strong interaction, especially with water molecules. As such, the cement hydration is probably hindered, reducing the concrete workability. Sugars, corn syrups, hydroxycarboxylic, acid, and lignosulfonates admixtures show similar phenomena with cement [2]. A 75 to 100 mm slump flow has medium workability [21]. Notably, understanding the NOCNF optimum concentration and its relationship to workability may be debatable.

Mechanical properties of the NOCNF concrete

The compressive and flexural strength of the reinforced concrete under uniaxial deformation after 7 and 28 curing days are presented in the bar charts in Figure 4A-D. Table 3 compares the flexural and compressive strength of the NOCNF concrete with reference materials from other cementitious systems. Higher mechanical properties were observed after 28 days compared to the 7 days of curing.

Compressive strength: From Figure 4A, the 0.05% and 0.10% NOCNF samples showed a 1.8% and 17.4% increase in compressive strength after 7 days and a 7.9% and 15.4% increase in strength after 28 days of curing, respectively. The compressive strength increases linearly with the NOCNF content, positively impacting the concrete mechanical performance. Figure 4B shows crack positions on the sides of the cube. No cracks were observed on the top and bottom planes for a 0.05% NOCNF sample. The compressive load constrained the movement of the plane on the top surface. The cracks on the cubes´ sides indicate a good brittle failure [22]. Higher CNF fractions of up to 0.3% were reported in previous studies without a significant improvement in mechanical properties [5,23,24]. Entanglements or agglomerations could be a problem at higher fractions for large-diameter nanofibrils such as microscale fibers. In contrast, the compressive data of the concrete reinforced with the apple CNF at a 1 wt.% fraction is higher [9]. For the current data, the compressive strength is unique with such a higher strength at a lower NOCNF fraction. While the compressive strength relates to other studies in the literature, we have demonstrated a comparable compressive strength at lower co. 0.1% NOCNF content. The higher compressive data from the literature on Kraft wood microfilament and cotton microcrystalline reinforced concrete came from a concrete mixture with fine aggregates. Mechanical data from microscale fibers such as banana fibers (5% fiber fraction) [4] and pine needles (0.5% fiber fraction) [25] at the same load fraction would probably be lower compared to the current data at 0.05% NOCNF content.

Flexural strength: Figure 4C presents the results of the flexural strength of NOCNF-reinforced concrete and the reference material. Figure 4D is the concrete sample at maximum deflection after failure. The flexural strength at 0.05% and 0.1% NOCNF increased from 3.25 to 6 MPa after 7 curing days, corresponding to an enhancement of 3.4%.

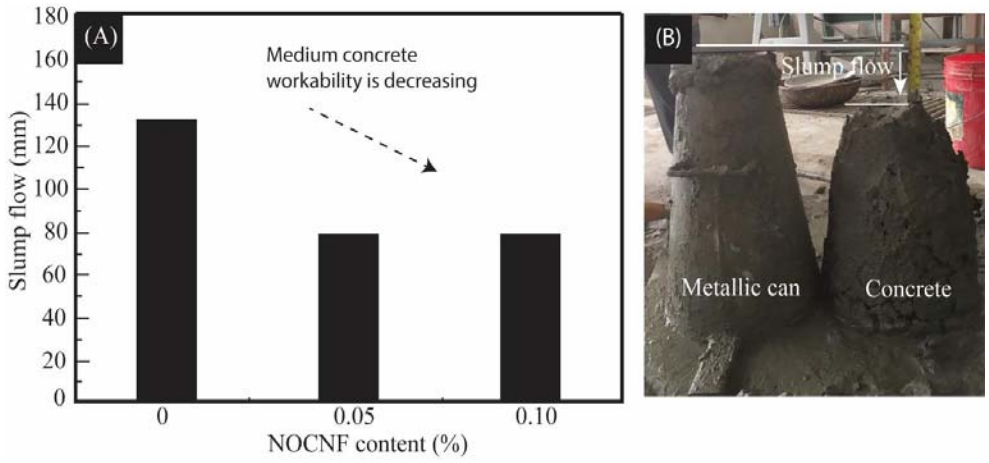

Figure 3: NOCNF-Concrete workability data (A) A bar chart of slump flow against NOCNF content (B) Slump test set up and a concrete flow at 0.05 % NOCNF content. The arrow points along the direction of the concrete flow.

Table 3: Flexural and compressive strength of reinforced concrete with NOCNF and reference materials from various sources.

S/N	Sample Description	CNF Content (%)	Nanofibril diameter (nm)	Curing time (days)	Flexural strength (MPa)		Compressive strength (MPa)		Ref.
					Reinforced concrete	% increase	Reinforced concrete	% increase	
1.	Banana rachis NOCNF + gravels + sand + cement	0.1	5.3	28	7.1(1.4)	12.7(0.7)	35.3 (1.9)	15.7	This study
2.	Apple CNF + gravels + sand + cement	1	2.7	28	5.7	35.7	43.7	12.7	[9]
3.	Cladophora algae CNF + sand + cement	5	37 – 55	28	6.0	173	-	-	[7]
4.	Kraft wood pulp cellulose microfilament + cement	0.2	30 – 400	28	5.8	20.6	76	26.1	[5]
5.	Cotton cellulose microcrystalline + sand + cement	0.04	> ~100	28	152	25.6	51	10.9	[6]
6.	Banana fibers + gravels + sand + soil + cement	5	142000	-	1.0	78.6	6.3	64	[4]
7.	Pine needle leaves + gravels + sand + cement	0.5	microscale	28	4.9	25.6	41.9	2.7	[25]

The flexural data reached 5 and 7.1 MPa, respectively, after 28 curing days, corresponding to an enhancement of 12.7%. The control sample with 0% NOCNF showed a higher flexural strength of 5.8 MPa than the 0.05% NOCNF samples at 7 and 28 days of curing. The lower flexural strength value at the lower NOCNF content is challenging. As stated, the plain concrete is brittle and sensitive to cracks under uniaxial tension. The presence of negatively charged carboxyl groups was expected to enhance the formation of a more rigid cementitious matrix. The flexural data are superior to other concrete with coarse aggregates and reinforced with CNF, for example, apple CNF-concrete [9]. The flexural strength of the concrete reinforced with MCC is much higher because of fine aggregates and superplasticizers.

Concrete shrinkage and porosity: Figure 4E presents shrinkage data, and Figure 4F is the porosity data associated with NOCNF content and the curing days. The shrinkage data of the 0.1% NOCNF sample is plotted with the reference material from a block of plain concrete. The concrete shrinkage increases with the number of curing days used in the experiment, up to 21 days. Initially, the 0.1% NOCNF sample shrank more in a liquid state than the plain concrete. Then, the shrinkage of the plain concrete and 0.1% NOCNF gradually coincide after 7 to 14 days. There is a linkage between higher shrinkage data and those of the compressive strength and flexural strength observed at 0.1% NOCNF fraction compared to that of the plain concrete, see Figure 4A,C. Notably, the block of NOCNF concrete shrunk 1.5 times compared to the plain concrete after the third day. Although the NOCNFs compete for the water molecules with the anhydrous cement particles, they also facilitate the formation of more CSH bonds [26]. The shrinkage characteristic around the first seven days deserves a detailed theoretical and experimental understanding beyond the scope of this work. The hydrophilic properties of cellulose were associated with dispatching the retained water to the cementitious matrix.

The porosity of the concrete mixture also decreases with increased NOCNF content, Figure 4F. The porosity of the 0.05% NOCNF sample is unusually high. The lower flexural properties of the 0.05% NOCNF compared to the plain concrete may be related to this higher porosity (Figure 4F,C). In addition, there is no appreciable difference in the

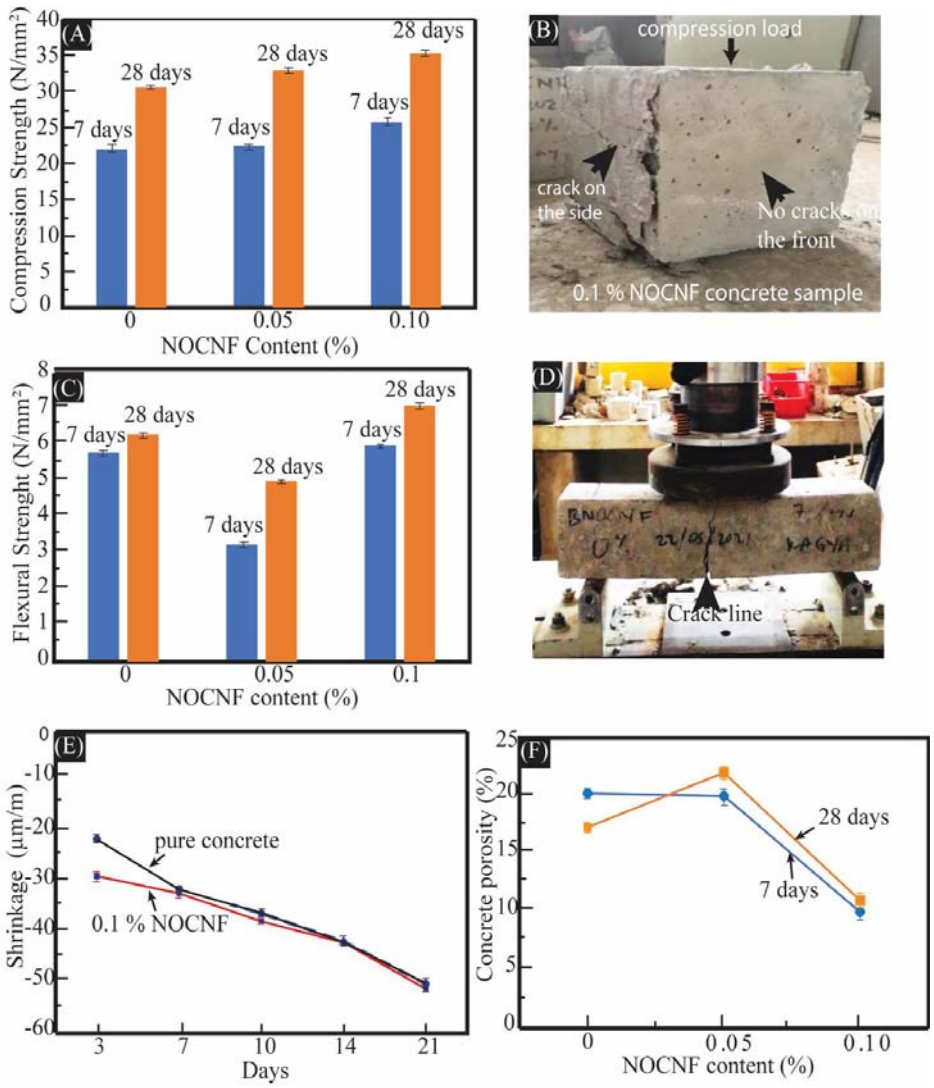

Figure 4: NOCNF-Concrete mechanical properties. (A) A bar chart of the relationship of NOCNF content to compressive strength (B) Compression cube after test indicating regions of a satisfactory compression failure zone of a 0.1% NOCNF concrete (C) A bar chart showing the relationship of NOCNF content to flexural strength (D) A flexural test setup and a plain concrete sample crack position under four-point bend test (E) A graph of concrete shrinkage against the number of curing days (F) The graph of a relationship between concrete porosity to the NOCNF content.

concrete porosity between 7 and 28 curing days. As such, the possibility of a nanostructured effect dominates, related to the NOCNF presence and the formation of CSH. The NOCNFs have an advantage due to their higher packing density in concrete [27-29], decreasing the porosity and increasing the probability of the nanofibrils intercepting micro-cracks in the cement matrix. Unfortunately, this work did not report the high-resolution microstructure examination to elucidate the presence of the nanostructured CSH and NOCNF in the concrete mixture.

X-ray powder diffraction of the NOCNF concrete

Figure 5 presents the XRD pattern of the pure NOCNF film, plain concrete, and 0.1% NOCNF concrete samples. A weak peak at 2theta = 15.4^{o} and a strong peak at 2theta = 22.6^{o} are apparently from the presence of cellulose I [30]. The plain concrete pattern demonstrates sharp peaks at 20.8^{o}, 26.7^{o}, and 29.7^{o} maxima. The peaks at 2theta = 10.2^{o} and 28.3^{o} are

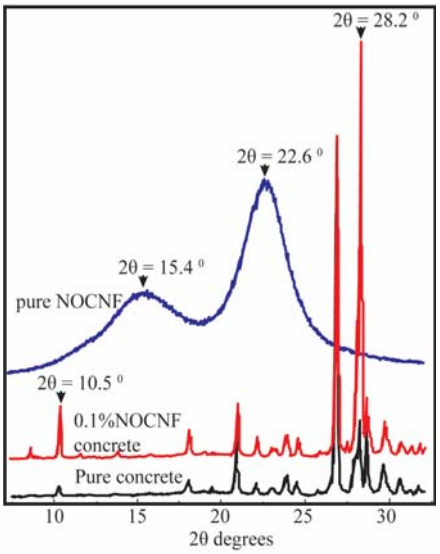

Figure 5: XRD Diffraction data of pure NOCNF film, plain concrete, and nanoengineered concrete with 0.1% NOCNF, cured at 28 days.

mainly present in the 0.1% NOCNF concrete mixture. The peaks from NOCNF at 15.2^{o} and 22.6^{o} disappeared in the diffraction pattern of a concrete sample, probably due to the dominant presence of the concrete phases. The diffraction pattern with sharp peaks at 2theta = 10.2^{o} and 28.3^{o} from the NOCNF concrete sample is difficult to understand. A typical diffraction pattern of a pure CSH phase shows peaks around 8.4^{o}, 29.9^{o}, 32.0^{o}, 35.7^{o} and 49.7^{o} [31]. Mohammadkazemi, et al. [32] observed an accelerated production of CSH during hydration with the addition of bacterial CNF. The data from the diffraction peaks of the concrete samples may be associated with CSH nanoparticles. Observing the typical CSH peaks is difficult compared to the reflection peaks from the pure CSH phase because of the concrete phase's distortion. In its crystalline forms, like tobermorite, CSH may show distinct peaks but is typically amorphous or nanocrystalline in concrete [33]. However, Ramachandran, Beaudoin [2], and El-Feky, et al. [6] associated higher water content regions in a concrete mixture with CH crystals rather than the CSH phase. With increasing cement particle stability in the presence of higher NOCNF content from our hydrocolloid images (Figure 2B), a strong argument probably favors forming a hydrated phase in the 0.1% NOCNF concrete samples. As such, the strong peak at 28.6^{o} may be associated with the formation of CH crystals, probably from amphibole, calcite, quartz, or aragonite, since a peak from the CSH hydrates is not apparent. The CH or CSH is carbonated to form aragonite or calcite upon exposure to carbon dioxide at high humidity [34]. Moreover, since XRD patterns are obtained using the concrete samples, and also knowing that almost 80% of the concrete volume consists of sand and gravel [35], the peaks at 2theta = 10.2^{o} and 28^{o} are probably related to the change inhomogeneity of the samples.

Limitations and future perspective of CNF application on concrete

The concept of incorporating CNF with small diameters into concrete to enhance its properties has been explored by Barknaut, et al. in 2019 [9]. The study utilized CNFs with a diameter of 2.3 nm obtained from apple peels. El-Feky, et al. [6] also emphasized the significant role of CNFs in improving the mechanical properties of concrete, particularly in enhancing its strength and durability. Our current study employed carboxylated CNF, specifically nitro-oxidized CNF, with a small diameter derived from banana rachis. However, there are two main limitations to consider. First, microstructure examination data on forming CSH are not reported. Understanding the relationship between structure and properties necessitates a better comprehension of the morphology and structure of the particles, which would complement the XRD and hydrocolloid data presented. The microscale fibers from biomass do not have a substantial effect on the properties of concrete. Second, integrating biomass, mainly using innovative nanotechnology approaches, into the construction industry has not been sufficiently explored. Though the authors have observed a significant improvement in flexural and compressive strength, fracture toughness, a parameter related to ductility, has not been investigated. An optimized study is needed, considering the effect of moisture content and curing time. A mechanistic model of an engineered concrete/CNF may be developed based on these findings. CNF is an appealing material due to its exceptional strength and stiffness compared to steel, Kevlar, carbon nanotubes, and glass fibers, all commonly used in construction. Furthermore, the surface hydroxyl groups can be modified to introduce functionalities, paving the way for smart concrete materials embedded with electronics and electrical components, such as temperature and humidity sensors, self-cleaning or self-repair mechanisms, and more.

Like apple peels, banana rachis is abundantly available from biomass waste. Both the study by Barknaut, et al. in 2019 [9] and our current study demonstrate the potential of biomass in technological applications. This idea is not only innovative but also holds significant promise for the future, especially given the majority of studies focusing on energy generation. The ongoing research in the literature [36] aims to integrate the biorefinery concept, where various components can be derived from biomass waste, including energy, nanofibrils, chemicals, and other valuable products like paper. Implementing this concept in the construction industry could yield far-reaching benefits. Furthermore, this topic aligns with the United Nations Charter goal number 17, promoting sustainable development, and is in line with Tanzania's strategic goals under the Tanzania Social Action Fund (TASAF) established in 2000 to eradicate poverty and reduce social inequalities [37]. This alignment with sustainability goals is a significant step towards a more sustainable future.

Conclusion

A low fraction of well-individualized NOCNF from banana rachis was employed to investigate the nanoscale effect on concrete's mechanical (compressive and flexural) properties in a hardened state. The study observed a substantial impact of the NOCNF on concrete properties. First, the cement paste was stabilized in water by adding a small NOCNF fraction. Second, the concrete with 0.1% NOCNF yielded better compression and flexural strength results for 28 days with a 16% and 13% increase compared to the 0.05 wt.% of NOCNF. The concrete porosity decreases with the increase in NOCNF content, which correlates to the mechanical properties. Thus, twofold may be a possible nanostructured effect on mechanical properties. One is associated with increased nanofibril packing at the bonding interface, supported by the shrinkage and porosity data of the 0.1% NOCNF sample. Second, the presence of the carboxyl groups (from the high degree of oxidation = 0.455 mmol/g) has an added advantage, combining the high strength and stiffness attributes of the NOCNF and the bonding strength from the cement hydration products such as CSH and CH. Higher mechanical performance is achieved using a low

fraction of NOCNF, a high-quality individualized nanofibril from the banana rachis. As a sustainable nanocomponent, the discussion about reducing the amount of cement in the concrete could be an attractive idea.

Acknowledgment

Mr. Edward Rwegasila is acknowledged for his assistance in preparing the nitro-oxidized cellulose nanofibrils. Dr. Qiong Wu is thanked for taking a high-resolution image through the Transmission Electron Microscope. The financial support from the Knut and Alice Wallenberg Foundation is highly acknowledged.

References

1. McCarthy MJ, Dyer TD. Pozzolanas and pozzolanic materials. In: Lea's Chemistry of Cement and Concrete. 5th ed. Amsterdam: Elsevier. 2019;363-467. Available from: https://discovery.dundee.ac.uk/en/publications/pozzolanas-and-pozzolanic-materials
2. Ramachandran VS, Beaudoin JJ. Handbook of analytical techniques in concrete science and technology: principles, techniques, and applications. Amsterdam: Elsevier; 2000. Available from: https://shop.elsevier.com/books/handbook-of-analytical-techniques-in-concrete-science-and-technology/ramachandran/978-0-8155-1437-4
3. Callister Jr WD. Materials science and engineering: an introduction. 7th ed. New York: Wiley; 2007. Available from: https://www.amazon.in/Materials-Science-Engineering-Introduction-Wiley/dp/0470120320
4. Mostafa M, Uddin N. Experimental analysis of Compressed Earth Block (CEB) with banana fibers resisting flexural and compression forces. Case Studies in Construction Materials. 2016;5:53-63. Available from: https://doi.org/10.1016/j.cscm.2016.07.001
5. Hisseine OA, Wilson W, Sorelli L, Tolnai B, Tagnit-Hamou A. Nanocellulose for improved concrete performance: A macro-to-micro investigation for disclosing the effects of cellulose filaments on strength of cement systems. Construction and Building Materials. 2019;206:84-96. Available from: https://doi.org/10.1016/j.conbuildmat.2019.02.042
6. El-Feky MS, El-Tair AM, Kohail M, Serag MI. Nano-Fibrillated Cellulose as a Green Alternative to Carbon Nanotubes in Nano Reinforced Cement Composites. International Journal of Innovative Technology and Exploring Engineering. 2019;8(12):2278-3075. Available from: https://www.ijitee.org/wp-content/uploads/papers/v8i12/L33771081219.pdf
7. Cengiz A, Kaya M, Bayramgil NP. Flexural stress enhancement of concrete by incorporation of algal cellulose nanofibers. Construction and Building Materials. 2017;149:289-95. Available from: http://dx.doi.org/10.1016/j.conbuildmat.2017.05.104
8. Rahimi-Aghdam S, Bažant ZP, Qomi MA. Cement hydration from hours to centuries controlled by diffusion through barrier shells of CSH. Journal of the Mechanics and Physics of Solids. 2017;99:211-24. Available from: https://doi.org/10.1016/j.jmps.2016.10.010
9. Barnat-Hunek D, ska-Chargot MS, Jarosz-Hadam M, Łagód G. Effect of cellulose nanofibrils and nanocrystals on physical properties of concrete. Construction and Building Materials. 2019;223:1-11. Available from: https://doi.org/10.1016/j.conbuildmat.2019.06.145
10. Senthilkumar K, Siva I, Rajini N, Jappes JW, Siengchin S. Mechanical characteristics of tri-layer eco-friendly polymer composites for interior parts of aerospace application. In: Sustainable composites for aerospace applications. Amsterdam: Elsevier. 2018;35-53. Available from: http://dx.doi.org/10.1016/B978-0-08-102131-6.00003-7
11. Moon RJ, Martini A, Nairn J, Simonsen J, Youngblood J. Cellulose nanomaterials review: structure, properties, and nanocomposites. Chemical Society Reviews. 2011;40(7):3941-94. Available from: https://pubs.rsc.org/en/content/articlelanding/2011/cs/c0cs00108b
12. Vincent JF, Wegst UG. Design and mechanical properties of insect cuticle. Arthropod Structure & Development. 2004;33(3):187-99. Available from: https://doi.org/10.1016/j.asd.2004.05.006
13. Florian TDM, Villani N, Aguedo M, Jacquet N, Thomas HG, Gerin P, et al. Chemical composition analysis and structural features of banana rachis lignin extracted by two organosolv methods. Industrial Crops and Products. 2019;132:269-74. Available from: https://dial.uclouvain.be/pr/boreal/object/boreal%3A214867/datastream/PDF_01/view
14. Zuluaga R, Putaux JL, Cruz J, Vélez J, Mondragon I, Gañán P. Cellulose microfibrils from banana rachis: Effect of alkaline treatments on structural and morphological features. Carbohydrate Polymers. 2009;76(1):51-9. Available from: https://doi.org/10.1016/j.carbpol.2008.09.024
15. Sharma PR, Joshi R, Sharma SK, Hsiao BS. A simple approach to prepare carboxycellulose nanofibers from untreated biomass. Biomacromolecules. 2017;18(8):2333-42. Available from: https://doi.org/10.1021/acs.biomac.7b00544
16. Chen H, Chi K, Cao R, Sharma SK, Bokhari SM, Johnson KI, et al. Nitro-oxidation process for fabrication of efficient bioadsorbent from lignocellulosic biomass by combined liquid-gas phase treatment. Carbohydrate Polymer Technologies and Applications. 2022;3:100219. Available from: https://doi.org/10.1016/j.carpta.2022.100219
17. Aïtcin P-C, Flatt RJ. Science and technology of concrete admixtures. Cambridge: Woodhead Publishing; 2015. Available from: https://shop.elsevier.com/books/science-and-technology-of-concrete-admixtures/aitcin/978-0-08-100693-1
18. Gligorovski S, Strekowski R, Barbati S, Vione D. Environmental implications of hydroxyl radicals (• OH). Chemical Reviews. 2015;115(24):13051-92. Available from: https://doi.org/10.1021/cr500310b
19. Rwegasila E, Li L, Berglund LA, Mushi NE. Strong nanostructured film and effective lead (II) removal by nitro-oxidized cellulose nanofibrils from banana rachis. Cellulose. 2024;31(5):1-17. Available from: http://dx.doi.org/10.1007/s10570-024-05749-4
20. International Organization for Standardization. Testing of concrete Part 3: Making and curing test specimens, ISO 1920. 2019. Available from: https://standards.iteh.ai/catalog/standards/iso/50dfd126-fd36-48c6-91d0-c3205fe2d4d8/iso-1920-3-2019?srsltid=AfmBOoqCGUljuxIj9MXyuQr5im8p13G5ItjrhVdC5CG_2C6M-rx8Tk7P
21. Lyons A. Materials for architects and builders. 3rd ed. Oxford: Butterworth-Heinemann; 2007. Available from: https://doi.org/10.4324/9780080465791
22. International Organization for Standardization. Testing of concrete — Part 4: Strength of hardened concrete, ISO https://cdn.standards.iteh.ai/samples/72260/a32f5d2f674047459842b873435fe9ee/ISO-1920-4-2020.pdf
23. Hisseine OA, Omran AF, Tagnit-Hamou A. Influence of cellulose filaments on cement pastes and concrete. Journal of Materials in Civil Engineering. 2018;30(6). Available from: http://dx.doi.org/10.1061/%28ASCE%29MT.1943-5533.0002287
24. Onuaguluchi O, Panesar D, Sain M. Properties of nanofibre reinforced cement composites. Construction and Building Materials. 2014;63:119-24. Available from: https://doi.org/10.1016/j.conbuildmat.2014.04.072
25. Long W, Wang Y. Effect of pine needle fibre reinforcement on the mechanical properties of concrete. Construction and Building Materials. 2021;278:122333. Available from: https://doi.org/10.1016/j.conbuildmat.2021.122333
26. Kolias S, Georgiou C. The effect of paste volume and of water content on the strength and water absorption of concrete. Cement and Concrete Composites. 2005;27(2):211-6. Available from: http://dx.doi.org/10.1016%2Fj.cemconcomp.2004.02.009
27. Cao Y, Zavaterri P, Youngblood J, Moon R, Weiss J. The influence of cellulose nanocrystal additions on the performance of cement paste. Cement and Concrete Composites. 2015;56:73–83. Available from: https://doi.org/10.1016/j.cemconcomp.2014.11.008

28. Flores J, Kamali M, Ghahremaninezhad A. An investigation into the properties and microstructure of cement mixtures modified with cellulose nanocrystal. Materials. 2017;10(5):498. Available from: https://doi.org/10.3390/ma10050498

29. Peters SJ, Rushing TS, Landis EN, Cummins TK. Nanocellulose and Microcellulose Fibers for Concrete. Transportation Research Record. 2010;2142:25–8. Available from: http://dx.doi.org/10.3141/2142-04

30. Nishiyama Y, Langan P, Chanzy H. Crystal structure and hydrogen-bonding system in cellulose Iβ from synchrotron X-ray and neutron fiber diffraction. Journal of the American Chemical Society. 2002;124 (31):9074-82. Available from: https://doi.org/10.1021/ja0257319

31. Guan W, Ji F, Chen Q, Yan P, Pei L. Synthesis and enhanced phosphate recovery property of porous calcium silicate hydrate using polyethyleneglycol as pore-generation agent. Materials. 2013;6(7):2846-61. Available from: https://doi.org/10.3390/ma6072846

32. Mohammadkazemi F, Doosthoseini K, Ganjian E, Azin M. Manufacturing of bacterial nano-cellulose reinforced fiber-cement composites. Construction and Building Materials. 2015;101:958-64. Available from: http://dx.doi.org/10.1016/j.conbuildmat.2015.10.093

33. Bergold S, Goetz-Neunhoeffer F, Neubauer J. Quantitative analysis of C–S–H in hydrating alite pastes by in-situ XRD. Cement and Concrete Research. 2013;53:119-26. Available from: https://doi.org/10.1016/j.cemconres.2013.06.001

34. Kezuka Y, Kawai K, Eguchi K, Tajika M. Fabrication of single-crystalline calcite needle-like particles using the aragonite–calcite phase transition. Minerals. 2017;7(8):133. Available from: http://dx.doi.org/10.3390/min7080133

35. Kong L, Gao L, Du Y. Effect of coarse aggregate on the interfacial transition zone of concrete based on grey correlation. Magazine of Concrete Research. 2014;66(7):339-47. Available from: https://doi.org/10.1680/macr.13.00269

36. Cherubini F. The biorefinery concept: Using biomass instead of oil for producing energy and chemicals. Energy Conversion and Management. 2010;51(7):1412-21. Available from: zhttps://www.scirp.org/reference/referencespapers?reference id=1864927

37. Tanzania Social Action Fund (TASAF). The United Republic of Tanzania. President's Office-State House. Available from: https://www.tasaf.go.tz/pages/test